PROCEEDINGS OF SCIENCE

Global LHC constraints on electroweak-inos with SModelS v2.3

Mohammad Mahdi Altakach,[a] **Sabine Kraml**,[a] **Andre Lessa**,[b] **Sahana Narasimha**,[c,d] **Timothée Pascal**,[a,*] **Théo Reymermier**[e] **and Wolfgang Waltenberger**[c,d]

[a] *Laboratoire de Physique Subatomique et de Cosmologie (LPSC), Université Grenoble-Alpes, CNRS/IN2P3, 53 Avenue des Martyrs, F-38026 Grenoble, France*

[b] *Centro de Ciências Naturais e Humanas, Universidade Federal do ABC, Santo André, 09210-580 SP, Brazil*

[c] *Institut für Hochenergiephysik, Österreichische Akademie der Wissenschaften, Nikolsdorfer Gasse 18, A-1050 Wien, Austria*

[d] *University of Vienna, Faculty of Physics, Boltzmanngasse 5, A-1090 Wien, Austria*

[e] *Université de Lyon, Université Claude Bernard Lyon 1, CNRS/IN2P3, Institut de Physique des 2 Infinis de Lyon, UMR 5822, F-69622, Villeurbanne, France*

E-mail: altakach@lpsc.in2p3.fr, sabine.kraml@lpsc.in2p3.fr, andre.lessa@ufabc.edu.br, sahana.narasimha@oeaw.ac.at, timothee.pascal@lpsc.in2p3.fr, t.reymermier@ip2i.in2p3.fr, walten@hephy.oeaw.ac.at

Electroweak-inos, superpartners of the electroweak gauge and Higgs bosons, play a special role in supersymmetric theories. Their intricate mixing into chargino and neutralino mass eigenstates leads to a rich phenomenology, which makes it difficult to derive generic limits from LHC data. We present a global analysis of LHC constraints for promptly decaying electroweak-inos in the context of the Minimal Supersymmetric Standard Model, exploiting the SModelS software package. Combining up to 16 ATLAS and CMS searches, we study what is the resulting exclusion power of the combination compared to the analysis-by-analysis approach.

ArXiv ePrint: 2312.16635

42nd International Conference on High Energy Physics (ICHEP2024)
18-24 July 2024
Prague, Czech Republic

*Speaker

PoS(ICHEP2024)296

1. Introduction

While experimental searches at the Large Hadron Collider (LHC) are typically pursued final state by final state, targeting specific (yet often unrealistic) simplified-model scenarios, global reinterpretations of the wealth of experimental results become more and more important in order to understand which scenarios are really excluded and where new physics may still be hiding. This is particularly true for searches for supersymmetry (SUSY), as SUSY phenomenology is extremely rich and realistic scenarios are expected to give signals in several different channels.

In this work, we perform a global analysis of LHC constraints for promptly decaying electroweak-inos (EW-inos) of the Minimal Supersymmetric Standard Model (MSSM) through global likelihoods. A global likelihood from the combination of different individual analyses is relevant for two reasons. First, the signal of a particular BSM scenario may be manifest in different final states, which are constrained by different analyses. Combining them uses more of the available data and thus provides more robust constraints. Second, experimental analyses can always be subject to over- or under-fluctuations in the data. In the former case, the observed limit is weaker, in the latter case stronger, than the expected limit. Again, the combination of different, approximately independent analyses can mitigate this effect and provide more robust constraints.

In this work, we exploit version 2.3 of the SModelS software package [1] and its large database of experimental results from Run 1 and Run 2 of the LHC. The set of experimental analyses used in this study consists of the 16 ATLAS and CMS publications, listed in Table 1, for which SModelS v2.3 can build a likelihood (3 from Run 1 and 13 from Run 2, with 9 being for full Run 2 luminosity). The following study is discussed in more detail in [2].

2. Electroweak-ino points and combination procedure

2.1 Electroweak-ino points

After EW symmetry breaking, the electrically neutral (charged) wino, bino and higgsinos mix together to give four neutralinos: $\tilde{\chi}^0_{1\ldots4}$ (two charginos: $\tilde{\chi}^\pm_{1,2}$), with the indices going from the lightest to the heaviest. In this work, the conservation of R-parity is assumed, meaning that at the LHC, SUSY particles can only be pair-produced, each of them must decay into an odd number of SUSY particles, and the lightest SUSY particle (LSP) is stable.

We intend to set constraints on the EW-ino sector of the MSSM by means of a random scan with flat priors. To this end, we generated around 100K model points by randomly scanning over the bino, wino, higgsino mass parameters M_1, M_2, μ, and the ratio of the Higgs vacuum expectation values $\tan\beta = v_2/v_1$, within the following ranges:

$$\begin{aligned} 10\ \text{GeV} < \quad M_1 \quad &< 3\ \text{TeV}, \\ 100\ \text{GeV} < \quad M_2 \quad &< 3\ \text{TeV}, \\ 100\ \text{GeV} < \quad \mu \quad &< 3\ \text{TeV}, \\ 5 < \quad \tan\beta \quad &< 50\,. \end{aligned}$$

All other SUSY breaking parameters were fixed to 10 TeV, assuming that the stop-sector parameters can always be adjusted such that $m_h \simeq 125$ GeV without influencing the EW-ino sector. The

ID	Run	lumi.	Final State ($+\not{E}_T$)	EMs ($+\not{E}_T$)	SRs	comb.
ATLAS-SUSY-2013-11	1	20.3	2 lept., 0 or $\geq$ 2 jets, 0b	$WW^{(*)}$	13	–
ATLAS-SUSY-2013-12	1	20.3	3 lept. (0–2 τ's), 0b	$WZ^{(*)}, Wh$	2	–
ATLAS-SUSY-2016-24	2	36.1	2–3 lept., 0 or $\geq$ 2 jets, 0b	WZ	9	–
ATLAS-SUSY-2017-03	2	36.1	2–3 lept., 0 or $\geq$ 1 jets, 0b	WZ	8	–
ATLAS-SUSY-2018-05	2	139	2 lept., $\geq$ 1 jets	$WZ^{(*)}$	13	pyhf
ATLAS-SUSY-2018-06	2	139	3 lept., 0 or 1–3 jets, 0b	$WZ^{(*)}$	2	–
ATLAS-SUSY-2018-32	2	139	2 lept., 0 or 1 jets, 0b	WW	36	pyhf
ATLAS-SUSY-2018-41	2	139	4 jets or $2b+2$ jets, 0 lept.	WW, WZ, Wh, Zh, ZZ, hh	3	SL
ATLAS-SUSY-2019-02	2	139	2 lept., 0 or 1 jets, 0b	WW	24	SL
ATLAS-SUSY-2019-08	2	139	1 lept., $(h \to) b\bar{b}$	Wh	9	pyhf
ATLAS-SUSY-2019-09	2	139	3 lept., 0 or $\geq$ 1 jets, 0b	$WZ^{(*)}$	20+31	pyhf
CMS-SUS-13-012	1	19.5	0 lept., $\geq$ 3 jets (q or b)	WW, WZ, ZZ	36	–
CMS-SUS-16-039	2	35.9	2+ lept., 0–2 hadr. τ's, 0b	$WZ^{(*)}$	11	SL
CMS-SUS-16-048	2	35.9	2 soft lept., $\geq$ 1 jets, 0b	WZ^{*}	12+9	SL
CMS-SUS-20-004	2	137	0 lept., $2\,h(\to b\bar{b})$	hh	22	SL
CMS-SUS-21-002	2	137	$\geq$ 2 AK8 jets, 0 or $\geq 1b$'s 0 lept.	WW, WZ, Wh	35	SL

Table 1: List of EW-ino analyses from LHC Run 1 ($\sqrt{s}$ = 8 TeV) and Run 2 (13 TeV) considered in this study. The column "lumi." gives the integrated luminosity in fb^{-1}. The column "comb." specifies whether and how signal regions (SRs) are combined: "pyhf" means a HistFactory model is used through interface with Pyhf; "SL" means that a covariance matrix is used; and "–" means only the most sensitive SR is used.

lower limits on M_2 and μ were chosen so as to avoid the LEP constraints on light charginos, while the bounds on $\tan\beta$ were chosen to avoid Yukawa couplings from becoming non-perturbatively large. The mass spectra and decay tables were computed with SOFTSUSY 4.1.11 [3], setting $m_h = 125$ GeV for consistency of the decay calculations.

We further select the points with only prompt decays, and we require $m(\tilde{\chi}_1^0) < 500$ GeV and $m(\tilde{\chi}_1^\pm) < 1200$ GeV in order to focus on the region which the current prompt EW-ino searches are sensitive to, leaving us with a total of 18247 points. The production cross sections are computed at next-to-leading order with Resummino 3.1.2 [4] if the leading-order ones are above 7×10^{-4} fb.

2.2 Combination procedure

The next step is to build a global likelihood from individual analysis likelihoods. Since we do not know inter-analyses correlations, only analyses that are approximately uncorrelated may enter the combination. The combined likelihood is then simply the product of the likelihoods of the individual analyses, as described in [1]. We assume analyses from different LHC runs, and from distinct experiments to be approximately uncorrelated. Furthermore, we also treat analyses which do not share any event in their SRs as approximately uncorrelated.

Since not all analyses in Table 1 can be combined with each other, many different combinations can often be built for each model point. Moreover, since the sensitivity of each individual analysis changes for each point, so does the sensitivity of any possible combination. Therefore, we dynamically determine for each point in the scan the most sensitive combination, defined as the one with the lowest expected upper limit on the signal strength μ (shared by all the individual likelihoods entering the combination). This (most sensitive) combination is then used to compute the expected and observed constraints, as well as the exclusion status of the point under consideration.

3. Results

The gain in expected reach due to the combination can be seen in the top left plot of Figure 1 for points with a bino-like LSP ($\tilde{\chi}_1^0 \geq 50\%$ bino). A point is expected to be excluded if an analysis gives $r_{\text{exp}} \equiv \sigma/\sigma_{\text{UL}}^{\text{exp}} \geq 1$, with σ the signal of the BSM model and $\sigma_{\text{UL}}^{\text{exp}}$ its expected upper limit at 95% confidence level. As anticipated, the expected reach is enhanced by the combination due to the accumulation of statistics, resulting in an overall increase of 48% in the expected number of excluded points (from 3081 to 4549). In the $m(\tilde{\chi}_1^\pm) \gtrsim 400$ GeV region, the expected exclusion is mostly driven by two analyses: the all-hadronic searches CMS-SUS-21-002 [5] and ATLAS-SUSY-2018-41 [6]. The points for which the most sensitive analysis is one of these two analyses are displayed by the blue and red histograms.

Turning to the observed exclusion (not shown here), the CMS hadronic search is less constraining than the ATLAS one. This is because the CMS and the ATLAS hadronic searches recorded over- and under-fluctuations, respectively. Consequently, the observed exclusion power of the CMS hadronic search is lower than what was expected, while it is the opposite for the ATLAS hadronic search. Overall, the number of excluded points increases by 35% with the combination.

In the top right plot of Figure 1, we show the impact of the analysis combination on the observed exclusion (a point is excluded if $r_{\text{obs}} \equiv \sigma/\sigma_{\text{UL}}^{\text{obs}} \geq 1$), compared to the most sensitive analysis (the one giving the highest r_{exp}), for points featuring a bino-like LSP. Only shown are the points which are not excluded by the most sensitive analysis but are excluded by the combination (orange and red), and the points which are excluded by the most sensitive analysis but are not excluded by the combination (blue). Most of the points observe a gain in exclusion power. This is because they feature a wino-like next-to-LSP (NLSP) and the analysis which is the most sensitive to these models (the CMS hadronic search) observed over-fluctuations; therefore, when combined with other analyses—which may have recorded under-fluctuations, as did the ATLAS hadronic search—the total observed exclusion increases significantly. Nevertheless, the opposite behaviour also occurs, see the blue points in this plot. These points are concentrated in a small region around $m(\tilde{\chi}_1^\pm) \simeq 900$ GeV and feature a higgsino-like NLSP. The most sensitive analysis in this region is the ATLAS hadronic search. The combination with other analyses again levels out much of these fluctuations, but this time results in a decrease of the exclusion power.

The bottom plots in Figure 1 show the points featuring a non-bino-like LSP.[1] From the bottom left plot we see that the ATLAS hadronic search is the most sensitive single analysis at high $m(\tilde{\chi}_2^\pm)$.[2] Consequently, in the bottom right plot, the exclusion power decreases for almost all points at high $m(\tilde{\chi}_2^\pm)$, and the combination excludes fewer points than the ATLAS hadronic search alone.

Figure 2 shows the points allowed by the combination ($r_{\text{obs}}^{\text{comb}} < 1$). The colour represents the $\tilde{\chi}_1^+$ wino content, quantified through the (1,1) component of the mixing matrix V defined as: $\left(\tilde{\chi}_1^+ \; \tilde{\chi}_2^+\right)^T = V\left(\widetilde{W}^+ \; \widetilde{H}_u^+\right)^T$, with $\widetilde{W}^+$ and $\widetilde{H}_u^+$ the positively charged wino and higgsino gauge eigenstates. For bino-like LSP points (left plot), purple points therefore correspond to models with a wino-like NLSP, while green points feature a higgsino-like NLSP. As expected, the allowed parameter space for points with a wino-like NLSP is smaller, due to their larger production cross sections. We also see that several points avoid exclusion at low masses if $m(\tilde{\chi}_1^0) \lesssim m(\tilde{\chi}_1^\pm)$. These points display mixed

[1] Mostly models with a higgsino-like LSP since those with a wino-like LSP typically have a long-lived $\tilde{\chi}_1^\pm$.

[2] For non-bino-like LSP points, $m(\tilde{\chi}_1^\pm) \approx m(\tilde{\chi}_1^0)$, so the relevant "heavy" mass scale is $m(\tilde{\chi}_2^\pm)$.

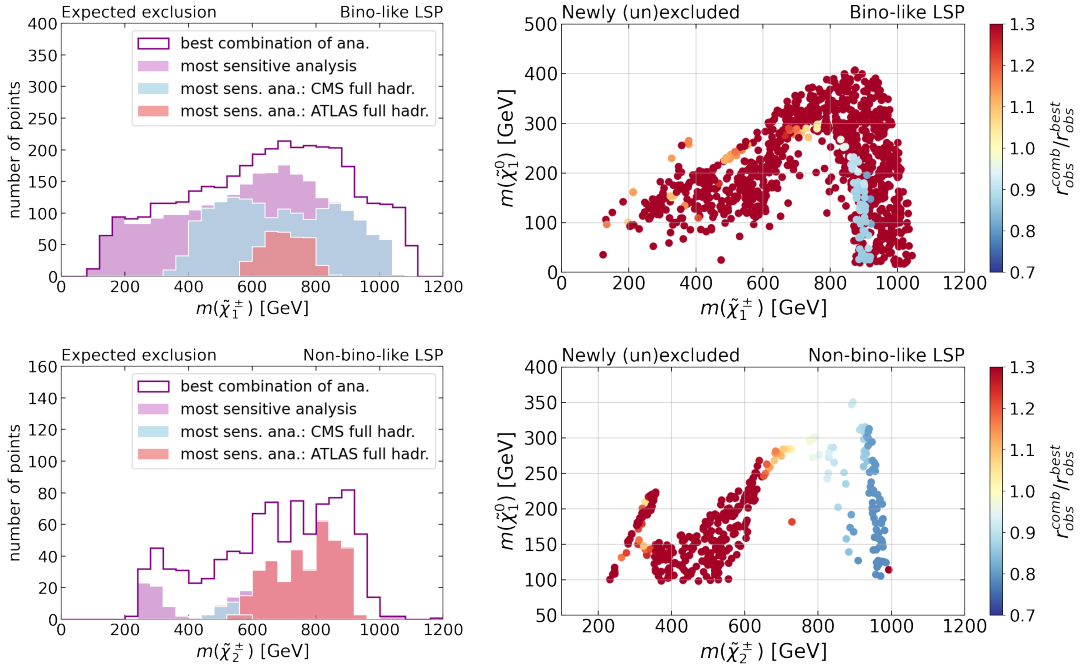

Figure 1: Comparison between the most sensitive analysis and the combination of analyses. The difference in sensitivity is shown in the left plots, while the right plots show the difference in exclusion power for the points that are only excluded by the combination (orange and red points), or that are excluded by the most sensitive analysis but not by the combination (blue points). The top plots show points with a bino-like LSP, while the bottom plots show points with a non-bino-like LSP.

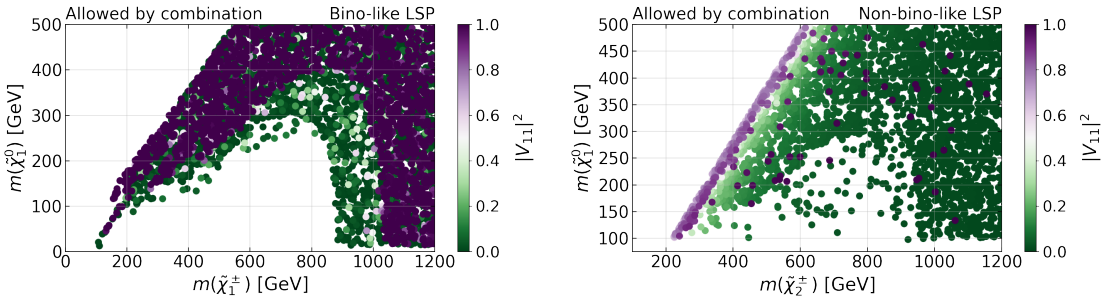

Figure 2: Points not excluded by the combination, with a bino-like LSP (left) and a non-bino-like LSP (right), identified by the wino admixture of the lightest chargino. Purple points correspond to scenarios where the lightest chargino is mainly wino-like, and green points to the scenarios where it is mainly higgsino-like.

scenarios, where the number of complex topologies is large, thus diluting the signal going into the simple 1-step decay topologies constrained by the database. The most important observation from the left plot of Figure 2 is, however, that there is a sizeable region which is definitely excluded. This region extends up to $m(\tilde{\chi}_1^\pm) \approx 900$ GeV for higgsino-like NLSP and up to $m(\tilde{\chi}_1^\pm) \approx 1$ TeV for wino-like NLSP. Such a region does not exist for non-bino-like LSP points, as shown in the right plot. Here, purple points correspond to models with a wino-like LSP, while green points feature a higgsino-like LSP.

4. Conclusions and outlook

Global LHC constraints on the EW-ino sector of the MSSM were obtained using SModelS v2.3. 16 ATLAS and CMS searches were combined in a dynamical global likelihood analysis. Around 18K points with promptly decaying EW-inos from a random scan over M_1, M_2, μ, and $\tan\beta$ were confronted against the experimental data (points with a long-lived chargino, typical of scenarios featuring a wino-like LSP, were not considered). For each point in the scan, the combination of analyses that maximises the sensitivity was determined, and the ratio of predicted over excluded cross sections (the so-called r-value in SModelS) computed.

The combination's impact on the expected reach and on the exclusion power was compared to that of the most sensitive analysis. We also showed how the combination in the high mass region is dominated by the two ATLAS and CMS hadronic searches, which recorded opposite fluctuations. All in all, the combination of analyses increases the number of points (expected to be) excluded by (48%) 35% compared to the most sensitive analysis. More importantly, it mitigates the sensitivity to fluctuations in the data, therefore leading to more robust constraints. Other interesting aspects, such as the identification of the various most sensitive combinations and how they populate the parameter space, the effect of the individual analyses on the global likelihood, and the combination's impact on the excess distribution are discussed in [2].

Let us finally highlight the crucial role of the reinterpretation materials for such a study. Some interesting experimental analyses could not be included in this work due to a lack of such materials. Indeed, a likelihood can only be built when efficiency maps and statistical models are available. We therefore acknowledge the collaborations' efforts in this direction and encourage them to continue publishing and preserving all valuable information necessary for reinterpretation studies.

Acknowledgments

The work presented here was funded in part by grants ANR-21-CE31-0023 (ANR; PRCI SLDNP), I 5767-N (FWF), ANR-15-IDEX-02 project no. G7H-IRG21B26 (IRGA; APM@LHC), 2018/25225-9 and 2021/01089-1 (FAPESP), and by the IN2P3 master project "Théorie – BSMGA".

References

[1] M.M. Altakach et al., *SciPost Phys.* **15** (2023) 185 [2306.17676].

[2] M.M. Altakach et al., *SciPost Phys.* **16** (2024) 101 [2312.16635].

[3] B.C. Allanach, *Comput. Phys. Commun.* **143** (2002) 305 [hep-ph/0104145]; B.C. Allanach et al., *Comput. Phys. Commun.* **220** (2017) 417 [1703.09717].

[4] B. Fuks et al., *JHEP* **10** (2012) 081 [1207.2159]; *Eur. Phys. J. C* **73** (2013) 2480 [1304.0790].

[5] CMS collaboration, *Phys. Lett. B* **842** (2023) 137460 [2205.09597].

[6] ATLAS collaboration, *Phys. sRev. D* **104** (2021) 112010 [2108.07586].